

See discussions, stats, and author profiles for this publication at: <https://www.researchgate.net/publication/6821321>

# Microfluidic Sequential Injection Analysis in a Short Capillary

ARTICLE *in* ANALYTICAL CHEMISTRY · OCTOBER 2006

Impact Factor: 5.64 · DOI: 10.1021/ac060714d · Source: PubMed

---

CITATIONS

36

---

READS

37

3 AUTHORS, INCLUDING:



Wenbin Du

Chinese Academy of Sciences

43 PUBLICATIONS 1,137 CITATIONS

SEE PROFILE



Qun Fang

Sun Yat-Sen University

95 PUBLICATIONS 1,292 CITATIONS

SEE PROFILE

# Microfluidic Sequential Injection Analysis in a Short Capillary

Wen-Bin Du, Qun Fang,\* and Zhao-Lun Fang

Institute of Microanalytical Systems, Department of Chemistry, Zhejiang University, Hangzhou, China

An automated microfluidic sequential injection analysis system that efficiently manipulates sample and reagent solutions in the nanoliter range in  $\sim 10$  s per analytical cycle is described. The system consisted of a 6-cm-long, typically 75- $\mu\text{m}$  i.d., fused-silica capillary (which functioned as a sampling probe and reactor as well as a flow-through detection cell), a horizontally oriented waste reservoir that provided liquid level differences for inducing gravity-driven flows, an autosampling device holding samples and reagents with horizontally fixed slotted microvials, and a laser-induced fluorescence detection system. Sample and reagent zones were sequentially introduced via gravity-driven flow by scanning the capillary tip (functioning as the sampling probe) through the vial slots, while vials containing sample, reagent, and carrier were sequentially rotated to the probe by programmed movement of the vial holders. Sequentially injected nanoliter zones were rapidly mixed by convection and diffusion within the carrier flow, demonstrating a behavior that conformed well to the Taylor dispersion model, and zone penetration effects were characterized and optimized under Taylor's dispersion theory guidelines. For the determination of fluorescein, a high throughput of 400  $\text{h}^{-1}$  was achieved, rapidly producing calibration curves (five points) within 45 s. Owing to its adaptability to the Taylor's dispersion model, the system was used also for measuring diffusion coefficients of fluorescent species. Potentials for using the system in enzyme inhibition assays were demonstrated by a reaction involving the conversion of fluorescein digalactoside to fluorescent hydrolysates via  $\beta$ -galactosidase and the inhibition of  $\beta$ -galactosidase by diethylenetriaminepentaacetic acid.

Sequential injection analysis (SIA),<sup>1,2</sup> as a new generation of flow injection analysis (FIA),<sup>3</sup> has now developed into a well-established technique enjoying broad acceptance, owing to improvements in the degree of automation, sample/reagent economy, and reliability, as compared to conventional FI systems. However, sampling frequencies are often degraded by at least a factor of 2 owing to the necessity of first sequentially aspirating

the sample and reagent zones via a multiposition valve into a holding coil before delivering the whole string into the reactor coil. Despite the reduction in sample/reagent consumption of SIA systems, in practice, usually at least a few hundred microliters is still required for a triplicate determination, including the volume involved in rinsing during sample change. Such levels of consumption are still often too excessive for valuable biosamples and biochemical reagents, so that lab-on-valve (LOV)<sup>4</sup> approaches were developed by Ruzicka's group to further reduce consumption as much as an order of magnitude through intensive integration of functional components on a multiposition valve. More recently, FIA performed in microfluidic formats using microfabricated chips was reported by several groups,<sup>5–9</sup> some with on-chip integration of functional components, such as pumps and valves,<sup>7</sup> but more often using conventional fluid-controlling means, such as syringe pumps and rotary valves for introducing samples and reagents into channels of a few micrometer depth.<sup>8,9</sup>

Except for LOV, effects on miniaturization of SIA are rarely reported. Davidsson et al. coupled a microfluidic chip with macroscale injection valves and pumps for construction of an enzyme-based microbiosensor with an optimal flow rate of 18  $\mu\text{L}/\text{min}$ .<sup>10</sup> Pu et al. recently reported a microchip-based electroosmotic flow pump that produced flow rates up to 1.5  $\mu\text{L}/\text{min}$ <sup>11</sup> and applied it with a six-way selection valve in a capillary-based SIA system for enzyme inhibition analysis. Gross sample consumption was reduced to  $<1 \mu\text{L}$ , but  $\sim 6$  min was required for each determination.

Recently, we reported a high-throughput nanoliter sample injection system,<sup>12</sup> which was composed of a capillary sampling probe connected with a microchip and an array of horizontally positioned microsample vials with a slot fabricated on the bottom of each vial. The system was used in a microchip-based FIA system employing a gravity fluid drive, achieving 1000  $\text{h}^{-1}$  high-throughput and with only 0.6–13-nL gross sample consumption. In this work, the slotted-vial array sample-injection system was combined with a short fused-silica capillary to produce a highly

\* To whom correspondence should be addressed. Phone: +86-571-88273496. Fax: +86-571-88273496. E-mail: fangqun@zju.edu.cn.

(1) Ruzicka, J.; Marshall, G. D. *Anal. Chim. Acta* **1990**, 237, 329.

(2) Gübeli, T.; Christian, G. D.; Ruzicka, J. *Anal. Chem.* **1991**, 63, 2407.

(3) Ruzicka, J.; Hansen, E. H. *Flow Injection Analysis*, 2nd ed.; John Wiley & Sons: New York, 1988.

(4) Ruzicka, J. *Analyst* **2000**, 125, 1053.

(5) Daykin, R. N. C.; Haswell, S. J. *Anal. Chim. Acta* **1995**, 313, 155.

(6) Hadd, A. G.; Jacobson, S. C.; Ramsey, J. M. *Anal. Chem.* **1999**, 71, 5206.

(7) Leach, A. M.; Wheeler, A. R.; Zare, R. N. *Anal. Chem.* **2003**, 75, 967.

(8) van Akker, E. B.; Bos, M.; van der Linden, W. E. *Anal. Chim. Acta* **1998**, 373, 227.

(9) Hofmann, O.; Miller, P.; Sullivan, P.; Jones, T. S.; deMello, J. C.; Bradley, D. D. C.; deMello, A. J. *Sens. Actuators, B* **2005**, 106, 878.

(10) Davidsson, R.; Genin, F.; Bengtsson, M.; Laurell, T.; Emnéus, J. *Lab Chip* **2004**, 4, 481.

(11) Pu, Q. S.; Liu, S. R. *Anal. Chim. Acta* **2004**, 511, 105.

(12) Du, W. B.; Fang, Q.; He, Q. H.; Fang, Z. L. *Anal. Chem.* **2005**, 77, 1330.

efficient and simple  $\mu$ SIA system that is capable of sequentially introducing hundreds of nanoliter sample/reagents at high throughputs without resorting to conventional valves and pumps. The downscaling effect of this  $\mu$ SIA system also resulted in a flow phenomenon that is in accordance with the Taylor dispersion model.<sup>13</sup>

## EXPERIMENTAL SECTION

**Chemicals.** All chemicals used were of reagent grade unless mentioned otherwise, and demineralized water was used throughout. Fluorescein was obtained from Sangon Biotechnology Co. (Shanghai, China), and a 50  $\mu$ M stock solution was prepared in water. A series of standard solutions was prepared by sequentially diluting the stock solution with water.

The enzyme reaction medium was 10 mM Tris buffer with a pH of 7.3 adjusted using 0.1 M HCl.  $\beta$ -Galactosidase ( $\beta$ -gal, *Escherichia coli*, 248 units/mg, Sigma, St. Louis, MO) was stored frozen and prepared in 10 mM Tris buffer with 0.10 mM  $MgCl_2$  at pH 7.3. The fluorogenic substrate fluorescein digalactoside (FDG) was obtained from Molecular Probes (Eugene, OR) and stored frozen as 10 mM stock solution in dimethyl sulfoxide (DMSO). The chemical pure inhibitor diethylenetriaminepentaacetic acid (DTPA, Nanxiang Reagents Co., Shanghai, China) was prepared and diluted with the same buffer.

**Capillary Preparation.** Fused-silica capillary (75  $\mu$ m i.d., Reafine Chromatography Co., Yongnian, China) was cut carefully with a cut stone, ensuring a flat end. The polyimide coating at the detection point and the probe tip of the capillary was removed carefully for a length of approximately 3 mm. The outer wall of the probe tip was silanized with dimethylchlorosilane (Guoyao Group Co., Shanghai, China) before use. For enzyme inhibition assay studies, a capillary with a secondary layer of polyacrylamide inside the bore (eCAP Neutral Capillary, Beckman Coulter, Fullerton, CA) was employed. The polyimide coating at the capillary tip was preserved for reducing adsorption of enzyme on the outer wall of the capillary.

**Slotted-Vial Autosampling Device.** The autosampling system consisted of a pair of gears driven by a programmed stepping motor and a set of horizontally fixed slotted vials, as presented in Figure 1. The slotted vials for containing samples and reagents were produced from 0.2-mL microtubes (Porex, Petaluma, CA) by fabricating 0.9-mm-wide, 1.0-mm-deep slots on the conical bottom of the tubes. The vials were fixed on a homemade vial-turning device produced from plastic gear parts. A gear pinion (12-tooth) disassembled from a used CD drive was fixed on the shaft of the motor, carrying a plate on which vials containing reagent and carrier solutions were installed. The pinion also served to drive another larger gear that held a plate for holding the sample vials. The tooth number of the larger gear (60-tooth or 72-tooth, custom-built, Qiushi Chemical Machine Factory, Hangzhou, China) was an integral multiple of the pinion to ensure the required precise relative positioning of sample and reagent/carrier vials during analytical cycles. A stepping motor driver equipped with an integrated pulse generator (custom-built, Sunrise Electric Co., Hangzhou, China) was used to control its movement using a program written in LabVIEW 8 (National Instruments, Austin, TX).

**$\mu$ SIA System.** A schematic diagram of the complete device is shown in Figure 1. Sample/reagent/carrier vials were fixed

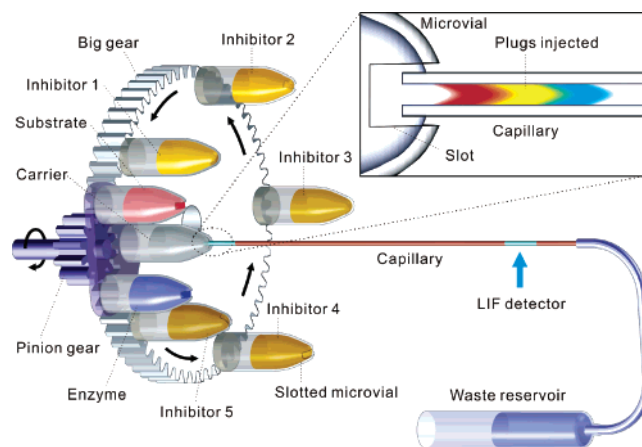


**Figure 1.** Schematic diagram of the  $\mu$ SIA system (not to scale, see the text for details).

horizontally at appropriate positions on the stepping-motor-driven autosampling device such that the vial slots could easily scan through the inlet end of the horizontally fixed capillary when the vials were rotated.<sup>14</sup> The outlet of the capillary was fixed and connected to a waste reservoir made from a 1-mL disposable syringe using a section of PVC tubing (40-cm long, 1.2-mm i.d.). The waste reservoir was horizontally fixed on a magnetic block to allow easy adjustment of the liquid level by sliding it along a scaled iron rod fixed in an upright position. The liquid level between the waste outlet and the capillary inlet provided the hydrostatic pressure required for the fluid drive in the microfluidic system.

On-column detection was achieved using a laser-induced fluorescence detector that was built as described in ref 15. The light beam of a 473-nm diode-pumped laser (10 mW, Changchun New Industries Optoelectronics Tech. Co., Changchun, China) was focused on the detection point of the capillary using a mirror-and-lens optical combination (40 $\times$  microscope objective lens, Chongqing MIC Optical & Electrical Instrument Co., Chongqing, China). The fluorescence signal was collected using a 25 $\times$  objective lens (Xi'an Sicong Laser Co., Xian, China) with an angle of 45° between the capillary and detection light path in the plane perpendicular to the laser beam,<sup>15</sup> followed by spatial filtering (0.9-mm diameter pinhole) and spectral filtering with a 520-nm band-pass filter (20-nm band-pass, HB Optical Technology Co., Shenyang, China). Collected fluorescence emission was measured using a CR114 photomultiplier tube (Hamamatsu, Beijing, China). Data acquisition was accomplished with a computer program written in LabVIEW.

**Procedures.** The automated operations are summarized in Figure 2. For studies using fluorescein as a model analyte (Figure 2, A1 and A2), the flow conduits and the waste reservoir were initially filled with water. The sample vials were manually filled with 200  $\mu$ L of a series of fluorescein standard solutions, with water filled in the carrier vial. The pinion carried a single carrier vial and turned 180° each time to switch between sample and carrier. Sampling/injection time (i.e., the stop period of the capillary inlet remaining in the sample vial slot) was set and precisely controlled by the computer, with pinion turning completed in 90 ms. For

(14) Fang, Q.; Du, W. B. Chinese Patent, Appl. No.: 200610049830.9, 2006.

(15) Fu, J. L.; Fang, Q.; Fang, Z. L. *Anal. Chem.* **2006**, *78*, 3827.

(13) Taylor, G. *Proc. R. Soc. (London)* **1953**, *219A*, 186.

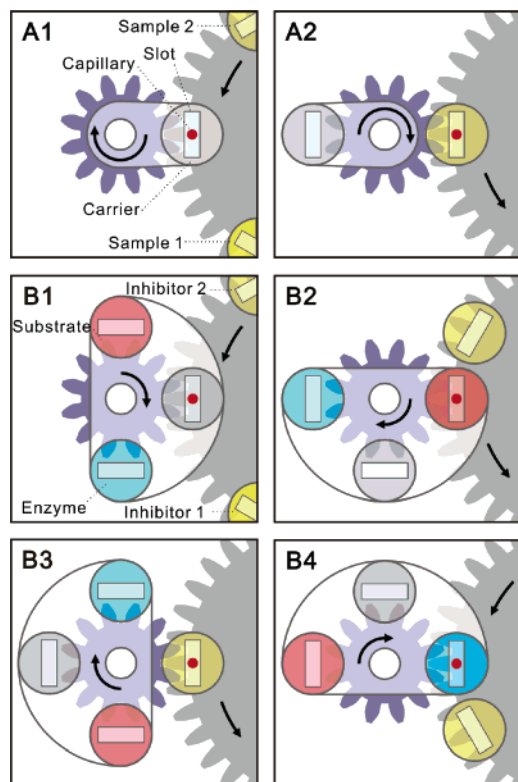


**Figure 2.** The sequential operations of the sample injection procedure (partial view of the autosampling device with the vial-holder plate on right). The red point denotes the position of the capillary probe end. A1 and A2 for fluorescein analysis with a small carrier vial-holder plate; A1, carrier; A2, sample. B1–B4 for enzyme inhibition assays with a larger multireagent vial holder; B1, carrier; B2, substrate; B3, inhibitor; B4, enzyme.

enzyme inhibition assays (Figure 2, B1–4), the three vials positioned each 90° apart on the plate fixed on the pinion were manually filled with substrate, carrier, and enzyme solutions, respectively. The sample vials on the plate of the larger gear were filled with 150- $\mu$ L inhibitor samples. For each analytical cycle, the pinion turned 360° clockwise in four sequences of 90° each, during which the vials scanned through the capillary in an order of carrier, enzyme, inhibitor sample 1, substrate, carrier, enzyme, inhibitor sample 2, substrate, etc., until all the samples on the sample vial holder were scanned. The sequentially injected train of solutions was transported through the capillary to the detection point and then to waste by the gravity drive. All experiments were performed at ambient room temperature of  $25 \pm 1$  °C.

For direct viewing and recording of the sample/reagent introduction process, a microscope (SZ-45B3, Sunny Instruments Co., Ningbo, China) equipped with a digital camera (DCMT130, Huaxin IC Technology Inc., Hangzhou, China) was used.

**Safety Considerations.** In setting up of the LIF detection system, dark glasses should be worn to avoid hurting of eyes by the laser beam.

## RESULTS AND DISCUSSION

### General Objectives and Considerations in System Design.

The first objective of this work was to improve the efficiency of SIA through miniaturization, in terms of both sample/reagent consumption and throughput. The second aim was to enhance

the predictability of SIA performance by realizing fluidic operations in the Taylor-flow region,<sup>13</sup> where the Gaussian distribution of an injected finite sample zone is largely predictable based on known experimental conditions. Microfabricated chip-based devices are now frequently adopted to achieve miniaturization and integration of flow analytical systems with significant reduction in analysis time and amount of sample. However, their efficiencies in terms of throughput (including sample changing) as well as gross sample consumption are far from being equally impressive. This deficiency is a consequence of inherent weaknesses in on-chip sample changing, which usually depends on on-chip reservoirs, and off-chip fluid drives. Furthermore, the optimization of flow conditions remains to be largely empirical, which is the result of the relatively complicated geometrical features of channel structures of microfabricated devices that are difficult to define mathematically. In this work, we used a single short fused-silica capillary tube combined with a slotted-vial rotating autosampling device to produce a very simple microfluidic system that could overcome the afore-mentioned deficiencies.

We showed in an earlier work<sup>12</sup> that high-throughput nanoliter sample injection for a microfluidic flow injection system could be achieved using a combination of a slotted-vial array and a capillary sampling probe with gravity fluid drive. Valveless sample injection was realized by simply scanning the capillary probe tip sequentially through the slots on the vials containing sample and carrier by linearly moving the vial array. Provided that the pressure drop of the gravity flow does not exceed a maximum value (discussed in detail later), surface tension at the capillary tip functioned as a valve during intervals between neighboring vials holding different solutions. When the tip was exposed to air, the flow was temporally stopped, and air entrainment was avoided. This simple approach was further developed in this work to allow the sequential injection of a number of reagent zones in addition to the sample and carrier to produce a simple SIA system without using pumps and valves. A further important improvement over the earlier design for the  $\mu$ FIA system was the development of a geared rotating holder for the carrier/reagent, synchronized to a similar but larger holder for multiple sample vials. With the geared system, only a single vial for the carrier solution (or other common reagents) was required instead of furnishing separate carrier solution vials between all neighboring samples, as in our previous work that featured a linear vial array design. A point that required special consideration with the present design was the gradual contamination of the carrier/reagents by the samples (and also among themselves) after multiple scanings of the capillary tip through the vials. To reduce such risks, the tip of the capillary was subjected to a hydrophobic treatment. The effects of such treatment are shown in the section entitled Analytical Performance.

With this design, as little as 20  $\mu$ L of sample in each vial proved to be sufficient for over 10 replications, and the remaining sample could be recovered for further work if precautions are taken to minimize carryover and cross-contamination. The gross consumption of samples could, therefore, be significantly reduced.

**Gravity-Driven Flow.** In the present  $\mu$ SIA system with gravity-driven flow, owing to requirements on maximum allowable capillary pressure drop ( $\Delta p$ ) of the gravity flow to ensure the valving function of the capillary tip, certain limitations are exerted



on the theoretical maximum flow rate. Analysis based on static equilibrium of surface-tension-induced pressure ( $p_s$ ) and gravity-induced pressure drop ( $\Delta p$ ) through the capillary is presented in eq1, and the maximum average velocity ( $v$ , cm/s) on the capillary can be given by eq2, known as Hagen–Poiseuille’s Equation.<sup>16</sup>

$$\left. \begin{aligned} p_s &= \frac{4\gamma}{d} \\ \Delta p &= \rho g \Delta H < p_s \end{aligned} \right\} \quad (1)$$

$$v = \frac{d^2}{32\mu} \cdot \frac{\Delta p}{l} \quad (2)$$

Here,  $\gamma$  denotes the surface tension (71.99 mN/m for water at 25 °C<sup>17</sup>),  $\rho$  is the density of the fluid,  $\mu$  is the viscosity of the solution, and  $l$  is the length of the capillary.  $p_s$  is the surface tension of the curved water–air interface, given by the Young–Laplace equation,<sup>18</sup> with the assumption that the tube wall has a wetting angle of 0°.  $\Delta p$  is the pressure drop generated by the difference in liquid levels ( $\Delta H$ ) between the sample/reagents/carrier vials and the waste reservoir.  $\Delta p$  should not exceed  $p_s$  to ensure almost immediate stopping of flow and preventing entrapment of air when the probe tip is exposed to air. As indicated, for a given capillary, the maximum flow rate is limited by the upper limit of  $\Delta p$  or  $\Delta H$ . For a  $\mu$ SIA system constructed using a 6-cm-long, 75- $\mu$ m-i.d. fused-silica capillary, according to these equations, the theoretical maximum  $\Delta H$  would be 39.2 cm, and the calculated maximum flow rate would be 57.4 nL/s. Experimentally, however, the liquid–air interface at the probe tip gradually turned unsteady when  $\Delta H$  exceed 30 cm.

**Taylor Dispersion Model in the  $\mu$ SIA System.** SIA systems are single conduit flow analysis systems based on sample and reagent mixing by convection and molecular diffusion. In conventional SIA, the optimum degree of zone mixing is mostly established experimentally, because flow conditions predominantly fall in the numerical flow region, where tailing peaks are commonly observed and behavior of injected sample zones is difficult to predict. Since the 1980s, several groups had been interested in establishing FIA based on Taylor dispersion,<sup>3</sup> in accordance with Taylor’s theory revealed in the 1950s,<sup>13</sup> in order to enhance the predictability of FIA performance through the scaling down of straight open tubular reactors.<sup>19–21</sup> However, various difficulties were encountered owing to lack of suitable injectors and detectors that can satisfy the degree of down-scaling required.<sup>21</sup> In this study, Taylor’s analysis of dispersion was used successfully to characterize the  $\mu$ SIA system, with the nanoliter injection system coupled to a thin straight capillary and low detection volume LIF detector, achieving good agreement between experimental results and theoretical calculations.

In the Taylor dispersion region, the dispersion of a finite solute zone in a straight capillary channel is mainly governed by axial

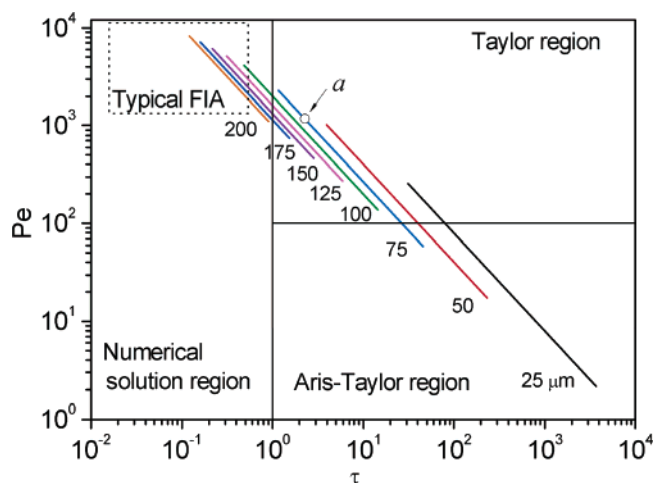


**Figure 3.** Regions of validity for different dispersion models. Colored lines: fluorescein dispersed in capillaries (i.d. from 25 to 200  $\mu$ m) with a reactor length of 5 cm. Point a: dispersion corresponds to 29.3 nL/s theoretical flow rate ( $\Delta H = 20$  cm) on 6-cm-long, 75- $\mu$ m-i.d. capillary.

convection and radial molecular diffusion, resulting in extended symmetric Gaussian shaped peaks with peak variance ( $\sigma_t$ ) expressed as<sup>22</sup>

$$\sigma_t^2 = \frac{d^2}{96D_m} t_v \quad (3)$$

where  $d$  denotes the inner diameter of the capillary,  $D_m$  is the molecular diffusion coefficient of the solute, and  $t_v$  is the residence time (time between the centers of sampling pulses and resulting peaks). Equation 3 shows that the band-broadening of Taylor flow is directly related to the residence time and can be readily controlled by adjusting the residence time. Thus, the degree of penetration of sequentially injected zones could be devised on the basis of known parameters. To do so, the use of a straight, thin, uniformly bored cylindrical tube as the only conduit is mandatory, and a few-centimeter section of fused-silica capillary used for capillary electrophoresis served the purpose well.

Regions of validity for different numerical solutions of dispersion could be mapped by two dimensionless numbers, Peclet number ( $Pe$ ) vs reduced time ( $\tau$ ) defined by eq4,<sup>21,23</sup> with the results as shown in Figure 3.

$$\left. \begin{aligned} \tau &= \frac{4t_v D_m}{d^2} \\ Pe &= \frac{v d}{D_m} \end{aligned} \right\} \quad (4)$$

Assuming fluorescein as a model solute, which has a diffusion coefficient of  $4.25 \times 10^{-6}$  cm<sup>2</sup>/s in water at 25 °C,<sup>24</sup> for 5-cm dispersion in a straight capillary with a definite inner diameter in the range of 25–200  $\mu$ m, the  $\tau$  and  $Pe$  values within the possible flow-rate range were calculated (maximum and minimum flow

(16) Nakayama, Y.; Boucher, R. F. *Introduction to Fluid Mechanics*; Arnold: London, 1999; p 93.

(17) *CRC Handbook of Chemistry and Physics*, 84th ed.; Lide, D. R., Ed.; CRC Press: Boca Raton, FL, 2004.

(18) Adamson, A. W.; Gast, A. P. *Physical Chemistry of Surfaces*, 6th ed.; John Wiley & Sons: New York, 1997; p 6.

(19) Tisjzen, R. *Anal. Chim. Acta* **1980**, *114*, 71.

(20) Hungerford, J. Ph.D. Thesis, University of Washington, Seattle, WA, 1986.

(21) van der Linden, W. E. *Trends Anal. Chem.* **1987**, *6*, 37.

(22) van den Berg, J. H. M.; Deelder, R. S.; Egberink, H. G. M. *Anal. Chim. Acta* **1980**, *114*, 91.

(23) Hull, R. D. Ph.D. Thesis, University of Cincinnati, Cincinnati, OH, 1993; p 4.

(24) Culbertson, C. T.; Jacobson, S. C.; Ramsey, J. M. *Talanta* **2002**, *56*, 365.

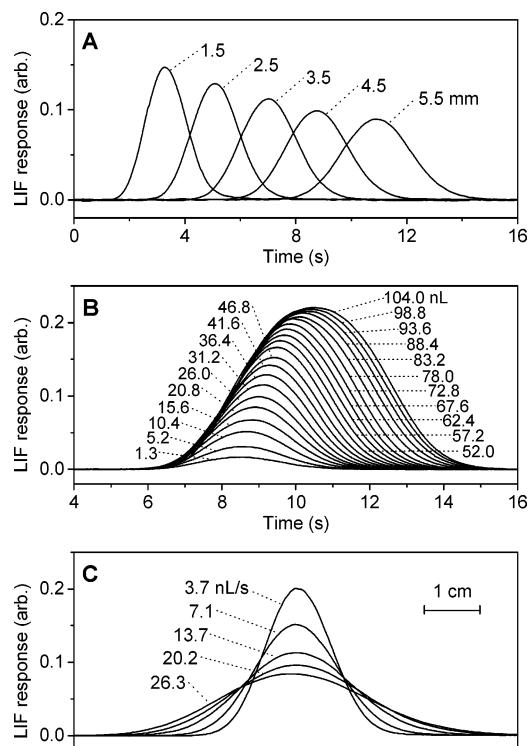


**Figure 4.** Influence of various factors on peak shape. A, effects of dispersion time in the range 3.3–10.9 s with a constant flow rate of  $22.3 \pm 0.5$  nL/s using a 7-cm-long, 75- $\mu$ m-i.d. capillary gained by varying the reactor length (capillary length from probe tip to detection point); B, effects of sample volume in the range 1.3–104 nL at a flow rate of 26.0 nL/s using a 6-cm-long, 75- $\mu$ m-i.d. capillary with 5-cm reactor length; C, effects of flow rate in the range 3.7–26.3 nL/s using capillary conditions the same as B. 100 nM fluorescein solution was employed as a model sample.

rates obtained according to eqs 1, 2 and  $\Delta H \geq 1$  cm), resulting in sloping lines corresponding to individual capillary inner diameters (as shown in Figure 3). These sloping lines show that downscaling of the inner diameter from 200  $\mu$ m to 25  $\mu$ m brings the system first from the numerical region into the Taylor area ( $Pe > 100$  and  $\tau > 1$ ), and further into the Aris–Taylor area.<sup>25</sup> The optimal inner diameter for a 6-cm-long capillary used in this work promising Taylor dispersion should be between 50 and 100  $\mu$ m.

The band broadening phenomenon based on Taylor's analysis of dispersion was investigated with a 75- $\mu$ m-i.d. capillary by injecting fluorescein sample plugs (100  $\mu$ M) at constant flow rates. With a 1-s sample injected ( $22.3 \pm 0.4$  nL volume) and the flow rate at 22.3 nL/s, the detection point was varied between 1.5 and 5.5 cm from the inlet of a 7-cm-long capillary (75- $\mu$ m i.d.), corresponding to residence time from 3.3 to 10.9 s. The effect of residence time on the dispersion is shown in Figure 4A. The peak width broadened almost linearly with an increase of residence time with a regression equation of  $w = 0.132t_v + 1.003$  ( $r^2 = 0.9929$ ), where  $w$  is  $2\sigma_v$ ,  $\sim 0.849$  the width of the peak at half-height. Small asymmetry could still be observed with  $t_v \leq 5.5$  s, but almost perfect symmetric peaks were obtained with an increase of  $t_v$ , indicating fulfillment of flow conditions in the Taylor dispersion region.

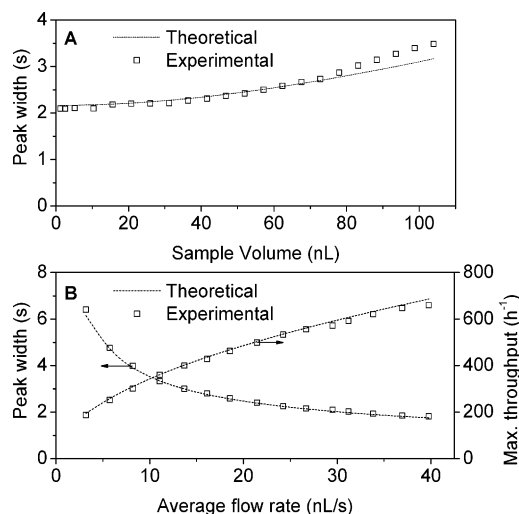


**Figure 5.** Effects of sample volume (A, extracted from Figure 4B) and flow rate (B) on peak width together with theoretical estimations using capillary conditions the same as in Figure 4B.

The effect of sample volume in the range 1.3–104 nL, corresponding to sample injection times of 0.05–4 s at 26.0 nL/s flow rate, is shown in Figures 4B and 5A on a 75- $\mu$ m-i.d. capillary with 5-cm reactor length. The results show a behavior similar to that in conventional FIA, but with almost symmetric peak shapes. As expected, the peak area was directly proportional to sample volume, and peak heights increased linearly within the range of 1.3 to 52 nL and then gradually sloped down to reach a platform at  $\sim 104$  nL.

The effect of flow rate on the peak width in the range of 3.7–26.3 nL/s is shown in Figure 4C. The peak width expressed in cm was calculated from the product of the peak width expressed in time (s) and individual flow rates (cm/s). Sample volume was controlled at  $20.8 \pm 0.4$  nL for each injection. As indicated by the figure, higher flow rates improved the maximum allowable throughput for the analysis and enhanced band broadening, which is beneficial for multizone penetration mixing.

Comparison of the experimental results with the theoretical data obtained using eq3 shows good agreement (Figure 5). Because the effect of injected volume on the peak width (at half peak height) was relatively small at volumes below 40 nL (Figure 5A), we chose an injection time of 1.0 s ( $25.4 \pm 0.5$  nL) to calculate the maximum allowable throughput for fluorescein at different flow rates. The results in Figure 5B show an inversely proportional decrease in peak width with an increase in the flow rate. The maximum throughput based on the supposition that two subsequent peaks should be at least  $6\sigma_t$  apart was estimated (Figure 5B). The calculated maximum sampling frequency of the  $\mu$ SIA system was 780  $h^{-1}$ , with the possibility of further enhancement by reducing the inner diameter and length of the capillary (as implied from eq 3), with some sacrifice in detection sensitivity. For example, theoretically, a 2.5-cm-long, 25- $\mu$ m-i.d. capillary with 2-cm dispersion distance would have a maximum throughput of more than 6000  $h^{-1}$ .

#### Characterization of Zone Penetration in the $\mu$ SIA System.

Mutual mixing of sample/reagent through zone penetration is essential for the successful execution of SIA systems.<sup>2</sup> The applicability of Taylor dispersion theory in the  $\mu$ SIA system allows easy optimization of parameters for efficient mixing through

(25) Aris, R. *Proc. R. Soc. (London)* **1956**, 235A, 67.

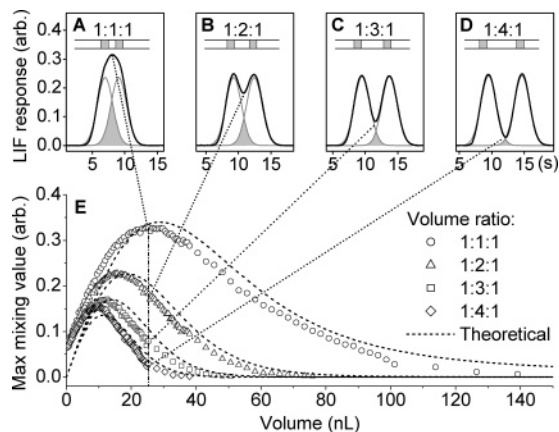


**Figure 6.** Penetration of two solute zones with increasing volumes of a third blank zone inserted between them using capillary conditions the same as in Figure 4B. A–D, peak shapes for three zones' mixing (two 1-s injected 250 nM fluorescein zones separated by a blank zone of 1, 2, 3, and 4 s); E, influence of zone volumes on the central mixing value of different ratios for three-zone sequential injections. Average flow rate, 25.3 nL/s.

dispersion. Mixing effects could be evaluated by the degree of penetration of two identical sample zones separated by a third blank zone with different volume ratios. As shown in Figure 6A–D, two 25-nL (~1-s injection) zones of fluorescein (0.25  $\mu$ M) separated by a blank zone of volumes from ~25 to 100 nL, produced peak shapes that changed from a single wide peak to two well-separated peaks. The optimal sampling (injection) volume for different volume ratios was studied by proportionally increasing the volumes of the three zones, keeping their ratios unchanged, and measuring the maximum degree of penetration at the isodispersion point,<sup>2</sup> appearing as peak maximums of the curves shown in Figure 6E. The theoretical curves calculated from Gaussian equations<sup>26</sup> derived for the two peaks according to Taylor's analysis of dispersion demonstrated very closely related trends similar to the experimental results. The reason for the small shift was that the calculations were made with the simplification that two peaks had the same Gaussian shape at the residence time when the signal was detected. More accurate prediction would require considerations in sample-volume-induced broadening and precise residence time of the two separated zones at the time of measurement.

**Analytical Performance.** Fluorescein was used as a model analyte to study the performance of the system. A typical recording for a standard series of 50–250 nM fluorescein is shown in Figure 7. The regression equation of peak height ( $I$ ) vs concentration ( $c$ ,  $\mu$ M) was:  $I = 0.0017c + 0.0004$  ( $r^2 = 0.9998$ ), exhibiting good linearity. The RSD of 1.0  $\mu$ M fluorescein was 0.8% ( $n = 7$ ). The sample consumption was 25 nL for each cycle. A high sample throughput of 400  $\text{h}^{-1}$  was obtained using injection times of 1 s for sample and 7.8 s for carrier.

In typical SIA systems, built from syringe pumps, holding coils and valves, some carryover between neighboring samples is almost unavoidable to maintain reasonable throughputs. In this work, owing to the extremely simple flow conduit, carryover effects in the capillary were easily avoided by running the carrier solution until sample peaks completely returned to baseline before

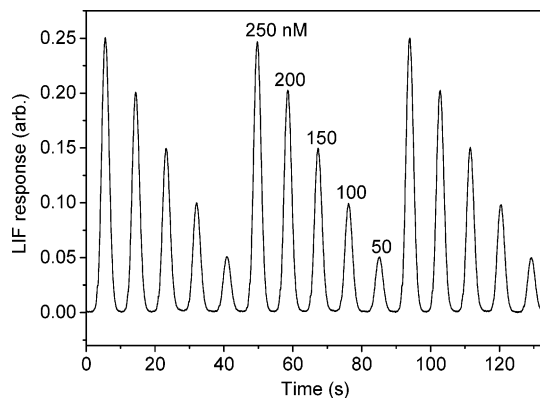


**Figure 7.** Typical recordings of fluorescein standard series on the capillary the same as Figure 4B. Concentration of the fluorescein for 1–5: 50, 100, 150, 200, and 250 nM. Injection time: 1 s fluorescein and 7.8 s carrier. Average flow rate, 25.0 nL/s.

injecting the next sample. The cross-contamination between neighboring vials was investigated by switching 1000 times between a 200- $\mu$ L fluorescein sample and a 200- $\mu$ L blank solution. Owing to the hydrophobic treatment of the capillary tip, a low total carryover of 0.15% was obtained after comparing the LIF response of the blank solution before and after the procedure.

**Determination of Diffusion Coefficient.** Ramsey's group<sup>24</sup> developed a microfluidic device for diffusion coefficient measurements based on static diffusion that required 2–8 min, depending on molecule size. More recently, Sharma et al.<sup>26</sup> presented a method for the rapid, efficient, and accurate measurement of the diffusion coefficient applying the Taylor dispersion model, using a commercial capillary electrophoresis (CE) instrument after taking into account the initial ramp in flow rate of such instruments. In this work, the good agreement of experimental results with theoretical estimations (using a reported diffusion coefficient of  $4.25 \times 10^{-6} \text{ cm}^2/\text{s}$ )<sup>24</sup> demonstrated in Figure 5B shows that our  $\mu$ SIA system has the potential of measuring diffusion coefficients using Taylor's dispersion model. The average diffusion coefficient of fluorescein calculated from sample peaks of 11.1–21.5-nL injected sample volume (1-s sampling time, as in Figure 5B) within a flow rate range of 11.1–21.5 nL/s was  $4.34 \times 10^{-6} \text{ cm}^2/\text{s}$  (RSD = 1.0%,  $n = 5$ ) calculated according to eq 3, which was very close to the reported value of  $4.25 \times 10^{-6} \text{ cm}^2/\text{s}$ .<sup>24</sup> The maximum throughput for the diffusion coefficient determination at the flow rate of 21.5 nL/s was 500  $\text{h}^{-1}$ .

**Enzyme Inhibition Assays.** A preliminary study on applying the  $\mu$ SIA system to enzyme inhibition assays was made using the present system to demonstrate its potentials in high-throughput drug discovery.<sup>27</sup> The assay was based on the inhibition of the  $\beta$ -galactosidase ( $\beta$ -Gal) enzyme by an inhibitor (in this case, DTPA), impeding the conversion of FDG to fluorescent hydrolysates, fluorescein-mono- $\beta$ -D-galactopyranoside (FMG) and fluorescein, via this enzyme.<sup>11</sup> The neutral capillary utilizes a secondary layer of polyacrylamide to generate a hydrophilic surface that can prevent  $\beta$ -Gal adsorption to the capillary walls. Optimization of experimental parameters was carried out with preliminary experiments on the effects of reaction rate, sample volume, and flow rate. Figure 8 displays the results of enzyme inhibition

(26) Sharma, U.; Gleason, N. J.; Carbeck, J. D. *Anal. Chem.* **2005**, *77*, 806.

(27) Maclean, D.; Schullek, J. R.; Murphy, M. M.; Ni, Z. J.; Gordon, E. M.; Gallop, M. A. *Proc. Natl. Acad. Sci. U.S.A.* **1997**, *94*, 2805.



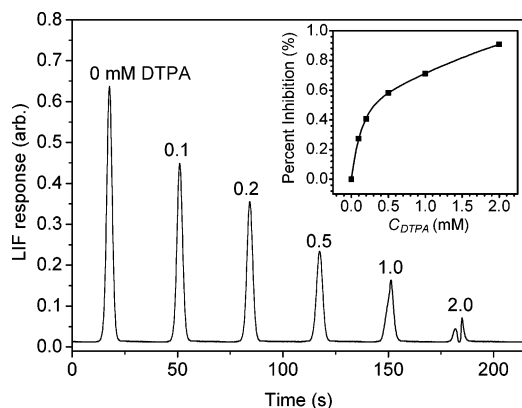


**Figure 8.** Typical recordings of enzyme inhibition assays obtained by varying the inhibitor (analyte) concentration while holding other conditions constant using a 6-cm-long, 50- $\mu$ m-i.d. capillary with 5-cm reactor length, obtained by sequentially injecting 1 s of  $\beta$ -Gal (0.1 mg/mL with 83  $\mu$ M  $\text{MgCl}_2$ ), 1 s of DTPA (0–2.0 mM), and 1 s of FDG (100  $\mu$ M); average flow rate, 4.2 nL/s. Percentage inhibition was calculated on the basis of peak area, according to ref 28.

studies, with a 6-cm-long, 50- $\mu$ m-i.d. capillary and a 15-cm difference between the liquid levels of the capillary and waste reservoir, which provided  $\sim 20$  s for achieving sufficient mixing and enzyme reaction. The net sample consumption was 4.2 nL for each determination. With enzyme and substrate zones separated by a DTPA solution with different concentrations from 0 to 2.0 mM, the reaction rate decreased due to the inhibition of DTPA on the activity of the enzyme, initially forming a tallest peak that was basically Gaussian, and at higher concentrations, producing a complete depression in the middle of the peak. With 100  $\mu$ M FDG, the percentage of inhibition<sup>28</sup> (PI) in the range of 0–2 mM DTPA was calculated on the basis of peak area, assuming the peak area of 0 mM DTPA to be 100% (i.e. 0% inhibition). The results are shown in Figure 8. A linear relationship was obtained between  $\log C_{\text{DTPA}}$  (mM) and percentage inhibition in the range of 0.1–2 mM DTPA, with a regression equation of  $\text{PI} = 0.476 \log C_{\text{DTPA}} + 0.738$ ,  $r^2 = 0.9932$ . The  $i_{50}$  value (inhibitor concentration required to produce 50% inhibition) was 0.32 mM DTPA. A precision of 2.7% RSD ( $n = 5$ ) was obtained for 0.5 mM DTPA, with a maximum possible throughput of 300  $\text{h}^{-1}$  deduced on the basis of the peak width.

## CONCLUSION

In the present work, a simple capillary-based microfluidic analysis system (CBMAS) was developed to perform SIA manipulation of multiple nanoliter volume liquids without resorting to complicated microfabrication techniques. Merging of laminar flows was avoided in this system so that mixing reactors<sup>29,30</sup> were not required to achieve efficient mixing. Taylor dispersion was found

to be sufficient for mixing of sequentially injected zones in performing reactions involving multiple reagents within a few seconds. The efficiency of the system was demonstrated not only in the high-throughput and low-sample/-reagent consumption but also in the automated sample change, a feature not always addressed in reported microfluidic systems, but nevertheless could be the real bottleneck for improving throughput in real applications.

A limitation of the present system is the relatively small volume available for detection, which could limit the sensitivity, an issue once considered by van der Linden about 20 years ago to be the ultimate obstacle for miniaturization before more sensitive detectors are available.<sup>21</sup> Although in this work this limitation was overcome by using an LIF detector, the fluorogenic properties of the sample/reagent posed a new limitation; however, we did show in an earlier work that sensitive spectrophotometric detection could be achieved in a nanoliter flow cell fabricated from Teflon AF to form a liquid core waveguide.<sup>12</sup> This approach is applicable to the  $\mu$ SIA system, although the predictability of dispersion characteristics based on Taylor's theory could be sacrificed somewhat owing to an unavoidable turn in the flow direction at the detector inlet. Although in the present work, no evident effects of the sample viscosity on system performance were observed for both fluorescein and  $\beta$ -galactosidase solutions, such matrix effects could occur when the viscosity of samples and standards do not match each other or when the viscosities of the samples are variable, especially for real life biosamples, such as serum. However, sample/standard viscosity variations could be readily overcome by appropriate calibration, which was easily and automatically conducted in the present system by periodically inserting matrix-matched standards into the vial array. Differences in sample viscosity can also be minimized by adding the same ratio of a viscous component (such as glycerol) to all samples and standards. We believe that the  $\mu$ SIA methodology developed in this work has great potential in bioanalysis involving precious samples and reagents, particularly those that involve the sequential mixing of several solutions. The approach also provides a powerful means for online process monitoring and high-throughput screening.

## ACKNOWLEDGMENT

Financial support from the National Natural Science Foundation of China (Grant 20575059) and National Education Ministry (Grant NCET-05-0511) are gratefully acknowledged. The authors also thank Jin-Lin Fu for help in the construction of the LIF detection device.

## SUPPORTING INFORMATION AVAILABLE

A video clip of the sequential sampling and mixing process of five dyes is available as Supporting Information. This material is available free of charge via the Internet at <http://pubs.acs.org>.

Received for review April 15, 2006. Accepted June 30, 2006.

AC060714D

(28) Hadd, A. G.; Raymond, D. E.; Halliwell, J. W.; Jacobson, S. C.; Ramsey, J. M. *Anal. Chem.* **1997**, *69*, 3407.

(29) Stroock, A. D.; Dertinger, S. K. W.; Ajdari, A.; Mezic, I.; Stone, H. A.; Whitesides, G. M. *Science* **2002**, *295*, 647.

(30) Seong, G. H.; Crooks, R. M. *J. Am. Chem. Soc.* **2002**, *124*, 13360.